HU 4329

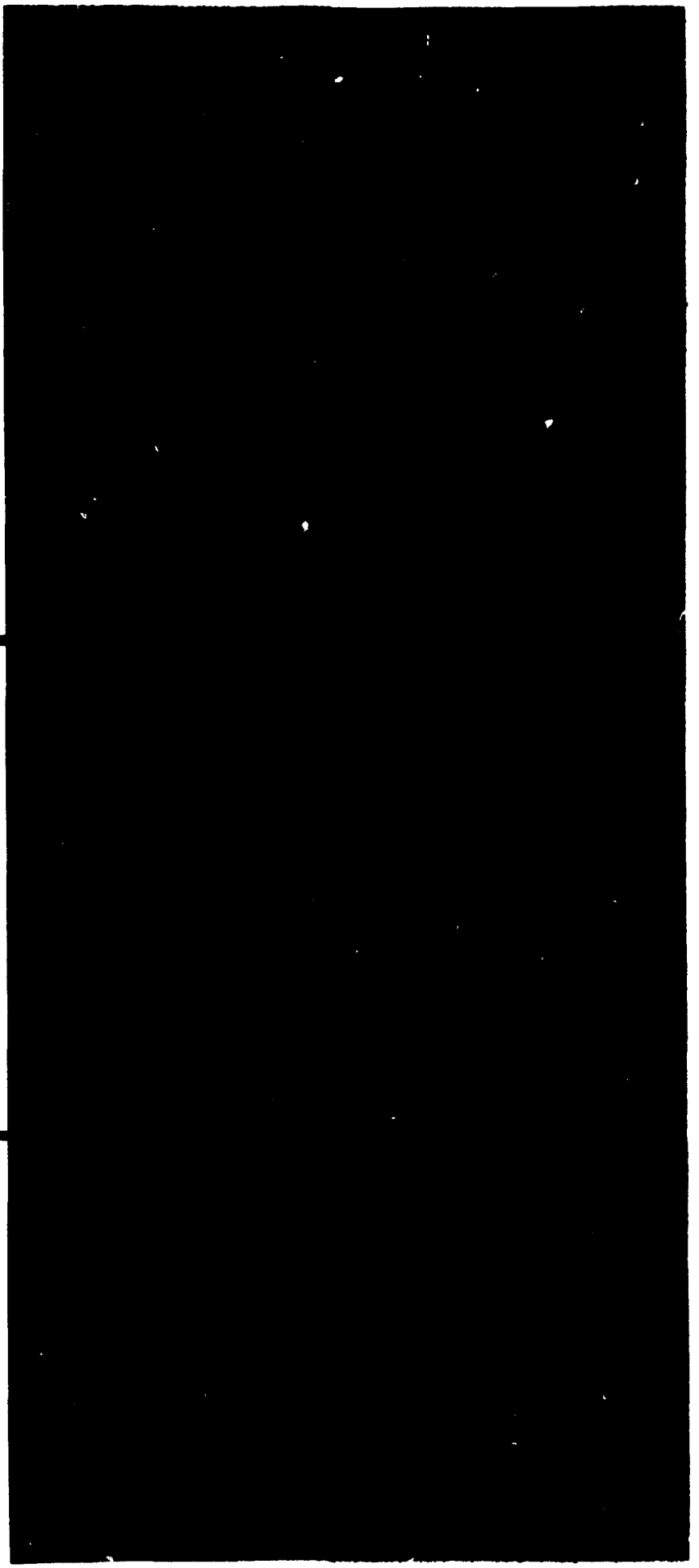

Á.Z. NAGY
B. VASVÁRI
P. DUWEZ
L. BAKOS
Z. SERES
J. BOGÁNCS
V.M. NAZAROV

KFKI-1979-91

VARIATION OF BORON CONCENTRATION IN METALLIC GLASS RIBBONS

Á.Z. Nagy, B. Vasvári, P. Duwez[+],
L. Bakos, Z. Seres, J. Bogáncs[x], V.M. Nazarov[x]

Central Research Institute for Physics
H-1525 Budapest, P.O.Box 49, Hungary

+ California Institute of Technology
Pasadena, California 91125, USA

x Laboratory of Neutron Physics
Joint Institute for Nuclear Research,
Dubna
Moscow, P.O.Box 79, USSR

Submitted to the Physica Status Solidi

HU ISSN 0368 5330
ISBN 963 371 618 7

ABSTRACT

The surface boron concentration of $Fe_{40}Ni_{40}P_{14}B_6$, $Fe_{32}Ni_{36}Cr_{14}P_{12}B_6$ and $Fe_{40}Ni_{40}B_{20}$ metallic glasses was measured by neutron activation analysis on both sides of the ribbon samples. It was found that the boron concentration is always higher at the bright side of the ribbon than that at the dull side which is in contact with the cold surface of the wheel during the rapid quenching from the melt. A possible explanation is given in terms of the solid-liquid interface moving rapidly from the cooled surface to the free surface when preparing the samples.

Range values of alpha-particles for some characteristic compositions of metallic glasses are tabulated.

A mathematical technique for the deconvolution of experimental data is described and the listing of the Fortran program is enclosed.

АННОТАЦИЯ

В работе определялось распределение бора в поверхностных слоях стекловидных материалов следующего состава: $Fe_{40}Ni_{40}P_{14}B_6$, $Fe_{32}Ni_{36}Cr_{14}P_{12}B_6$ и $Fe_{40}Ni_{40}B_{20}$. Эксперименты показали, что концентрация бора на блестящей стороне всегда больше концентрации матовой стороны. Во время быстрого охлаждения матовая сторона непосредственно прикасается к поверхности охлаждающего барабана. Можно предположить, что переходная жидкотвердая фаза находилась в быстром передвижении в процессе затвердевания.

Для некоторых стекловидных материалов даны значения пробега альфа-ча ниц в виде таблицы.

Описывается математическая программа деконволюции для обработки данных и прилагается программа для БЭСМ-6 на языке FORTRAN.

KIVONAT

$Fe_{40}Ni_{40}P_{12}B_6$, $Fe_{32}Ni_{36}Cr_{14}P_{12}B_6$ és $Fe_{40}Ni_{40}B_{20}$ összetételü fémüveg szalagok felületi bórkoncentrációját mértük a szalag mindkét oldalán. Azt találtuk, hogy a bórkoncentráció mindig magasabb a szalag fényes oldalán, mint a matt oldalán. A matt oldal van a henger hideg felszinével kapcsolatban, az olvadékból történő gyors lehütés során. Feltehető, hogy a szilárd-folyadék átmeneti réteg gyors mozgásban van a hideg oldalról a szabad felszin felé a megszilárdulási folyamat alatt.

Néhány jellemző összetett üvegfémre táblázatosan megadjuk az alfa-részecskék hatótávolság értékeit.

Leirjuk a mérési adatok dekonvolúciójánál használt matematikai eljárást és mellékelten csatoljuk a Fortran nyelven irt programot, melyet BESZM-6 számitógépen futtattunk.

INTRODUCTION

Recently a growing interest has been shown in a new type of material known as metallic glass or amorphous metal [1]. The reason is that this material has properties which are promising for practical applications and, at the same time, a new field has been opened up for fundamental research. A large group of metallic glasses are alloys of composition $Tm_{100-x}M_x$, where TM represents one or more transition metal elements like Fe, Ni, Cr, Pd, Pt, and M represents metalloid atoms like B, C, Si, P [2]. The composition range is usually x = 15-25 at% for the metalloid elements. The properties of metallic glasses are usually strongly influenced by the concentration of metalloid elements therefore it is important to know how accurately we can control the metalloid content of the ribbons along their length and cross sections.

In this paper we present results of neutron activation analysis measurements of B concentration in ribbons of $Fe_{40}Ni_{40}P_{14}B_6$ /Metglas^R sample a/, $Fe_{32}Ni_{36}Cr_{14}P_{12}B_6$ /sample b/ and $Fe_{40}Ni_{40}B_{20}$ /sample c/. The cross sections of the ribbons were 29x0.052, 6x0.046, and 0.55x0.020 mm^2, respectively. Samples /a/ and /b/ were provided by the Allied Chemical Co. /Morristown/, sample /c/ by Bell Laboratories /Murray Hill/; the provision of these samples is gratefully acknowledged.

EXPERIMENTAL

The applied analytical procedure is based on the nuclear reaction $^{10}B/n, \alpha/^7Li$. The details of the method used were described in a previous work [3]. The sample is placed into a thermal neutron beam and during the irradiation time the number of α particles released in the nuclear reaction as well as their energy losses are measured. The concentration profile measurements are non-destructive and there is no need to use the surface layer removal technique. Due to the relatively large /3840 barns/ cross section of the nuclear reaction mentioned the determination of B concentration can be made in practically any alloy without interference. The measurements were carried out with the IBR-30 pulsing reactor of the Joint Institute for Nuclear Research, Dubna, using the time-of-flight technique with a thermal neutron flux of $10^6 n/cm^2.s$. The length of the ribbon sample was usually 40 mm and in the case of narrow samples more pieces were placed near each other in order to increase the surface under investigation. The measured values for B concentration should be

treated as average quantities over a surface of 100-600 mm^2. Every 100 mm^2 surface of the samples was irradiated by 10^{11} thermal neutrons, so the detection limit was about 10^{-7} g of natural boron. For monitoring the flux thin films of ^6LiF were used and an accuracy of $\pm$ 1 % in flux measurement was achieved. For the two sides of the ribbon two independent measurements were carried out and the measured values were corrected by monitor counts. The reproducibility was $\pm$ 4 % with a sample containing 1 mg boron and repeating the measurements ten times. As a standard a compound with given boron concentration was evaporated onto an aluminium substrate with a thickness of a few tens of nm.

The energy loss, ΔE, suffered by an α-particle created by the neutrons at distance R from the surface of the sample can be measured, and the number of α-particles with energy loss ΔE should be proportional to the number of B atoms at distance R from the surface. The connection between ΔE and R is given by the expression

$$R = \int_{E_o}^{E_o-\Delta E} \left(\frac{dE}{dx}\right)^{-1} dE \quad , \tag{1}$$

where dE/dx is the stopping-power for alpha particles and the primary energy E_o = 1471 keV. This can be calculated for metallic glasses in a semiempirical way by using the stopping cross section data /ϵ_α/ of ref. [4] for the elements of the samples

$$\epsilon_\alpha = \frac{dE}{d\rho_A} = \frac{1}{N}(dE/dx) = \sum_{n=0}^{5} a_n E_o^n \quad , \tag{2}$$

where $(dE/d\rho_A)$ is the energy loss per unit surface density (atom/cm^2), N is the number of atoms per cm^3 in the sample, a_n are coefficients of the energy-polynomial valid in the range 400 keV $\leq E_o \leq$ 4000 keV. The unit of ϵ_α is eV/(10^{15} atoms/cm^2). For composite materials or mixtures Bragg's addition rule can be used; this states that the stopping powers are additive:

$$\epsilon_{comp} = C_A\epsilon_A + C_B\epsilon_B + C_C\epsilon_C + C_D\epsilon_D \quad , \tag{3}$$

where C_A, C_D and ϵ_A, ..., ϵ_D are the concentrations and the stopping cross sections for the elements A, ... D, respectively.

In separate Tables in this paper the R values obtained in the way described are collected for some characteristic compositions of metallic glasses in the range of energy losses of ΔE = 1 keV-300 keV, which corresponds to a depth of about 0.5 μm. The validity of the addition rule used in calculating the relation between R and ΔE is not discussed here. Interested readers are advised to consult earlier papers [4, 5]. We obtained previously quite reasonable results by remeasuring known boron concentration distributions; /see *Fig. 4*/. We thus hope that the above approach is not too far from reality in the case of metallic glasses.

RESULTS

In *Figs. 1-3* the boron-concentration profiles of the samples can be seen as a function of the depth up to 0.5 μm measured from the two opposite surfaces of the ribbon films. *Fig. 1* shows the results for sample /a/ along its length proving that there is no appreciable variation in boron concentration with respect to this direction. *Figures 2* and *3* correspond to samples /b/ and /c/, respectively.

The lower part of the figures /the dotted line/ shows the number of counts for α-particles above the background level with respect to the channel number /i.e. the energy scale/. Actually this is the energy-distribution of the emitted α-particles. The upper part of the figures /the continuous line/ shows the calculated natural boron concentration as a function of the depth measured from the surfaces.

The boron concentration is slightly increases with depth in the measured alpha-spectra. This small increase is probable not a real effect in the boron profile, but it is much better due to the effect of alpha-straggling which was neglected in our present work.

It is a real effect, however, and well within our experimental error, that the boron concentrations on the right hand side of the figures, which correspond to the bright side of the ribbon, are always higher than those on the left. It is well-known that during the preparation of the samples by rapidly cooling the liquid alloys, the bright side is a free surface whereas the dull side is connected with the cold surface of the rotating wheel.

The difference in boron concentration between the two surfaces of the ribbon is probably due to the heat gradient which is present in the sample during the rapid cooling.

Similarly to slowly cooled crystalline alloys, the solidification process involves the motion of a solid-liquid interface from the surface of the ribbon in contact with the wheel to the outside /bright/ surface. In slowly cooled alloys the interface is relatively thick and the concentration of alloying elements either increases or decreases, according to the equilibrium diagrams. In rapid cooling, the thickness of the solid-liquid interface must be very small and the temperature gradient very large, but such an interface must exist even if it is as thin as a few atomic distances. Within such a thin layer, diffusion can take place very rapidly since it involves a few atomic jumps only. In the case of Fe-B alloys, if it is assumed that the boron atom is thermodynamically more stable in the liquid than in the solid state, there is a tendency for boron to be "swept" to the liquid side of the ribbon with the advancing solid-liquid interface. This is a process similar to that in zone melting, the main difference being the very thin liquid-solid interface which results in very short diffusion distances and apparently high diffusion rates.

It is noticeable that in some cases, e.g. sample /b/, we got considerably smaller boron concentrations at both sides than we expected from the nominal values.

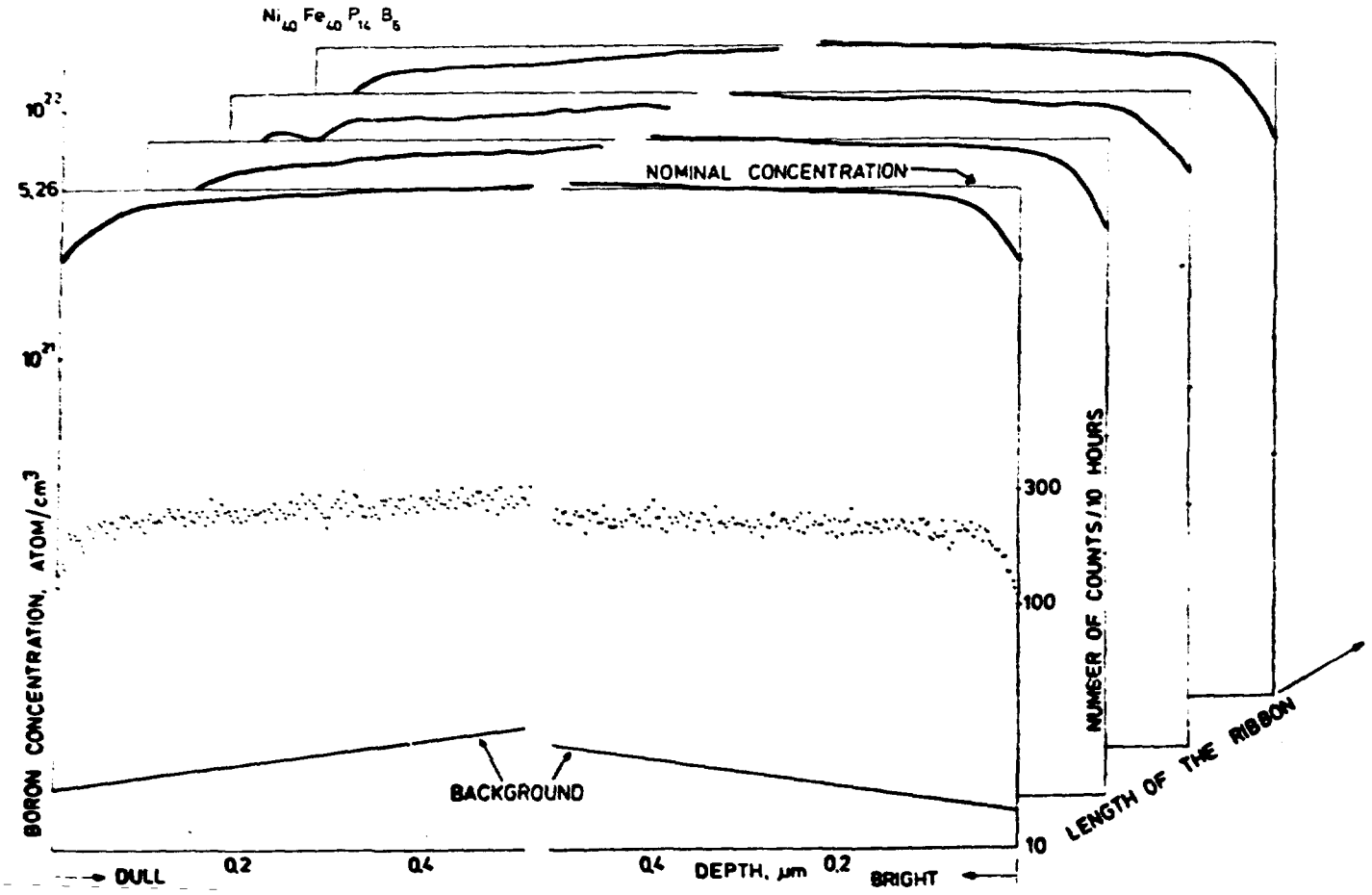

Fig. 1

Boron concentration depth distribution in $Ni_{40}Fe_{40}P_{14}B_6$ glassy metal ribbon. The dotted line - the measured alpha spectrum; the continuous line - the calculated concentration distribution. The distribution according to length refers to approximately 10 metres of ribbon

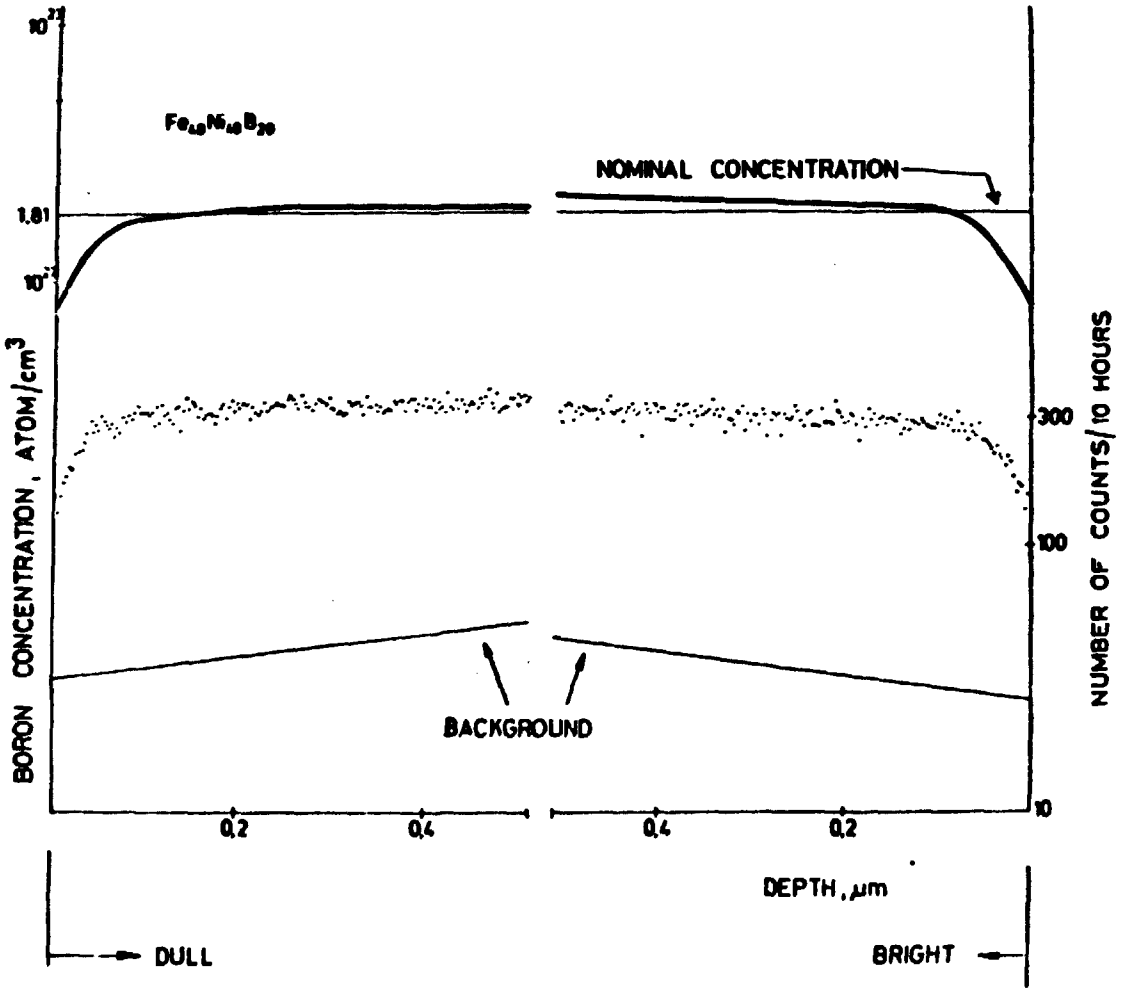

Fig. 2

Boron concentration depth distribution in $Fe_{40}Ni_{40}B_{20}$ glassy metal ribbon. The dotted line - the measured alpha spectrum; the continuous line - the calculated concentration distribution

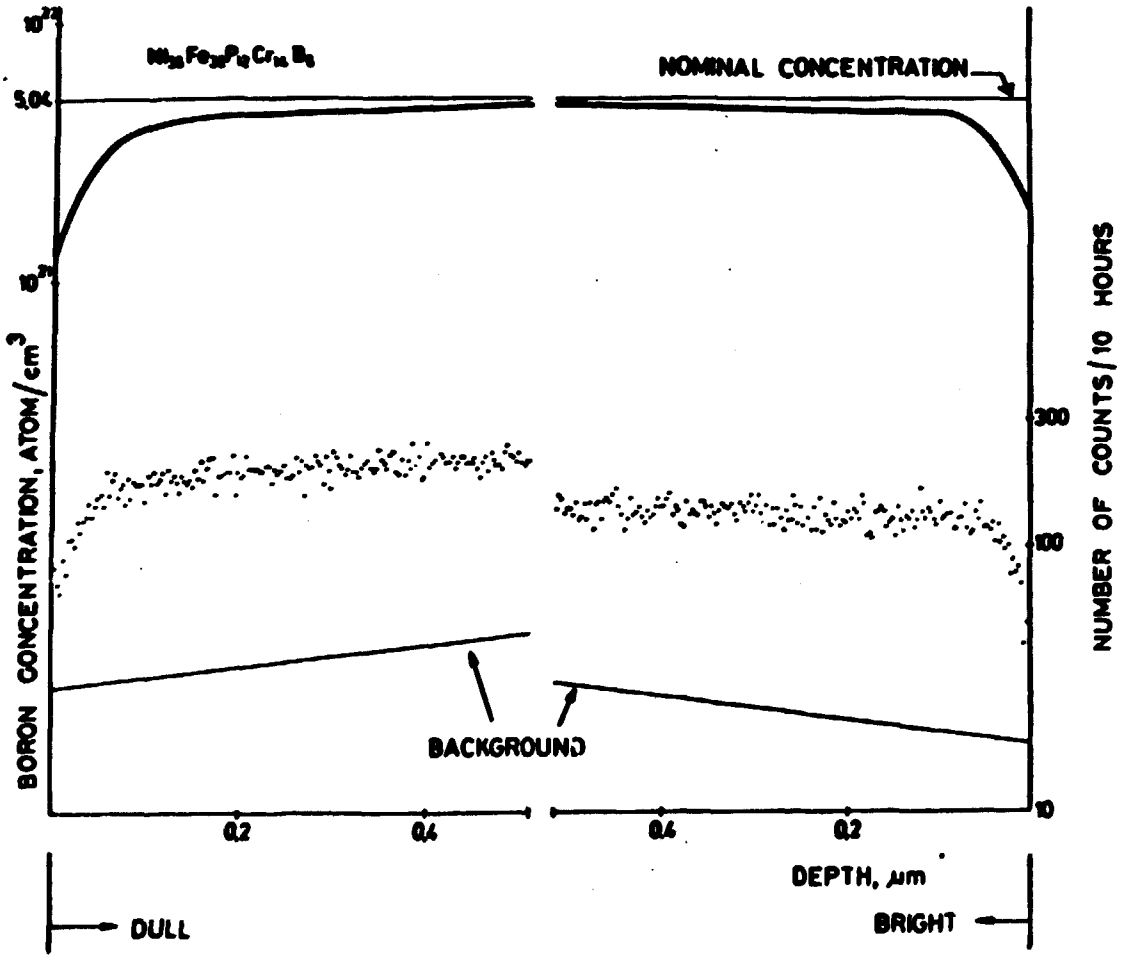

Fig. 3

Boron concentration depth distribution in $Ni_{36}Fe_{32}P_{12}Cr_{14}B_6$ glassy metal ribbon. The dotted line - the measured alpha spectrum; the continuous line - the calculated concentration distribution

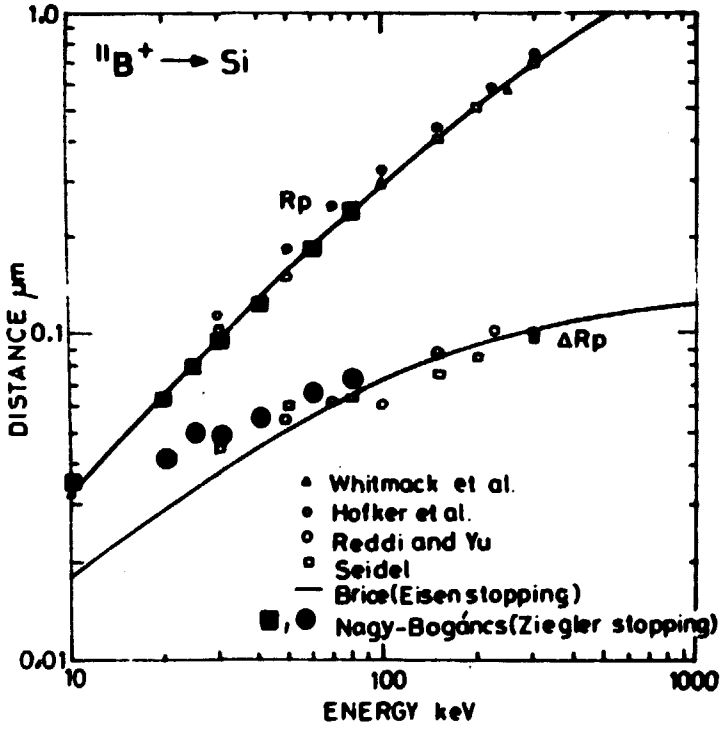

Fig. 4

The projected range (R_p) and the longitudinal standard deviation (ΔR_p) of ^{10}B atoms implanted into silicon. This measurement demonstrates the validity of Ziegler stopping [4] in the range from 0.03 to 0.35 μm. For additional details, see ref. [3]

T A B L E S

FOR DEPTH CALCULATION FROM ENERGY LOSS ACCORDING TO EQ. (1)

In these tables (Tables I-VI) the range values of alpha-particles are collected for different composite metallic glasses. R is expressed in μm and the energy loss ΔE increases from 1 keV to 300 keV by 1 keV steps from the starting energy E_o = 1471 keV. Let us see an example. If we determine 300 keV energy loss in the Metglas® sample this refers to 0.482 μm and as a comparison we shall get 0.990 μm in silicon sample under the same conditions

Table	Material	Density
I	$Fe_{40}Ni_{40}P_{14}B_6$	7.4
II	$Fe_{32}Ni_{36}Cr_{14}P_{12}B_6$	7.1
III	$Fe_{40}Ni_{40}B_{20}$	7.2
IV	$Fe_{80}B_{20}$	6.8
V	$Fe_{83}B_{17}$	6.9
VI	Si_{100}	2.33

Table I R values for $Fe_{40}Ni_{40}P_{14}B_6$

ΔE =	1	2	3	4	5	6	7	8	9	10
0	1.6968E-03	3.3948E-03	5.0891E-03	6.7827E-03	8.4746E-03	1.0170E-02	1.1862E-02	1.3554E-02	1.5245E-02	1.6939E-02
	1.8625E-02	2.0314E-02	2.2002E-02	2.3689E-02	2.5376E-02	2.7062E-02	2.8748E-02	3.0432E-02	3.2118E-02	3.3800E-02
20	3.5482E-02	3.7164E-02	3.8845E-02	4.0526E-02	4.2206E-02	4.3885E-02	4.5563E-02	4.7241E-02	4.8918E-02	5.0596E-02
	5.2270E-02	5.3945E-02	5.5620E-02	5.7293E-02	5.8966E-02	6.0638E-02	6.2310E-02	6.3981E-02	6.5651E-02	6.7321E-02
40	6.8990E-02	7.0658E-02	7.2326E-02	7.3993E-02	7.5659E-02	7.7325E-02	7.8990E-02	8.0654E-02	8.2318E-02	8.3981E-02
	8.5643E-02	8.7305E-02	8.8966E-02	9.0626E-02	9.2286E-02	9.3945E-02	9.5603E-02	9.7261E-02	9.8918E-02	1.0057E-01
60	1.0223E-01	1.0389E-01	1.0554E-01	1.0719E-01	1.0883E-01	1.1050E-01	1.1213E-01	1.1380E-01	1.1548E-01	1.1710E-01
	1.1879E-01	1.2043E-01	1.2208E-01	1.2370E-01	1.2535E-01	1.2699E-01	1.2864E-01	1.3028E-01	1.3193E-01	1.3357E-01
80	1.3521E-01	1.3686E-01	1.3850E-01	1.4014E-01	1.4178E-01	1.4342E-01	1.4506E-01	1.4670E-01	1.4834E-01	1.4998E-01
	1.5161E-01	1.5325E-01	1.5489E-01	1.5652E-01	1.5816E-01	1.5979E-01	1.6142E-01	1.6306E-01	1.6469E-01	1.6632E-01
100	1.6795E-01	1.6958E-01	1.7121E-01	1.7284E-01	1.7447E-01	1.7610E-01	1.7773E-01	1.7935E-01	1.8098E-01	1.8261E-01
	1.8423E-01	1.8586E-01	1.8748E-01	1.8910E-01	1.9073E-01	1.9235E-01	1.9397E-01	1.9559E-01	1.9721E-01	1.9883E-01
20	2.0045E-01	2.0207E-01	2.0369E-01	2.0531E-01	2.0693E-01	2.0854E-01	2.1016E-01	2.1177E-01	2.1339E-01	2.1500E-01
	2.1662E-01	2.1823E-01	2.1984E-01	2.2144E-01	2.2307E-01	2.2468E-01	2.2629E-01	2.2790E-01	2.2951E-01	2.3112E-01
40	2.3273E-01	2.3434E-01	2.3594E-01	2.3753E-01	2.3916E-01	2.4076E-01	2.4237E-01	2.4397E-01	2.4558E-01	2.4718E-01
	2.4878E-01	2.5038E-01	2.5199E-01	2.5359E-01	2.5519E-01	2.5679E-01	2.5839E-01	2.5999E-01	2.6159E-01	2.6319E-01
60	2.6478E-01	2.6638E-01	2.6798E-01	2.6957E-01	2.7117E-01	2.7276E-01	2.7436E-01	2.7595E-01	2.7755E-01	2.7914E-01
	2.8073E-01	2.8232E-01	2.8392E-01	2.8551E-01	2.8710E-01	2.8869E-01	2.9028E-01	2.9187E-01	2.9345E-01	2.9504E-01
80	2.9663E-01	2.9822E-01	2.9980E-01	3.0139E-01	3.0298E-01	3.0456E-01	3.0614E-01	3.0773E-01	3.0931E-01	3.1090E-01
	3.1248E-01	3.1406E-01	3.1564E-01	3.1722E-01	3.1880E-01	3.2038E-01	3.2196E-01	3.2354E-01	3.2512E-01	3.2670E-01
200	3.2828E-01	3.2985E-01	3.3143E-01	3.3301E-01	3.3458E-01	3.3616E-01	3.3773E-01	3.3931E-01	3.4088E-01	3.4246E-01
	3.4403E-01	3.4560E-01	3.4717E-01	3.4874E-01	3.5032E-01	3.5189E-01	3.5346E-01	3.5503E-01	3.5660E-01	3.5816E-01
20	3.5973E-01	3.6130E-01	3.6287E-01	3.6444E-01	3.6600E-01	3.6757E-01	3.6913E-01	3.7070E-01	3.7226E-01	3.7383E-01
	3.7539E-01	3.7696E-01	3.7852E-01	3.8008E-01	3.8164E-01	3.8320E-01	3.8477E-01	3.8633E-01	3.8789E-01	3.8945E-01
40	3.9101E-01	3.9257E-01	3.9412E-01	3.9568E-01	3.9724E-01	3.9880E-01	4.0035E-01	4.0191E-01	4.0347E-01	4.0502E-01
	4.0658E-01	4.0813E-01	4.0969E-01	4.1124E-01	4.1279E-01	4.1435E-01	4.1590E-01	4.1745E-01	4.1900E-01	4.2055E-01
60	4.2211E-01	4.2366E-01	4.2521E-01	4.2676E-01	4.2831E-01	4.2985E-01	4.3140E-01	4.3295E-01	4.3450E-01	4.3605E-01
	4.3759E-01	4.3914E-01	4.4068E-01	4.4223E-01	4.4378E-01	4.4532E-01	4.4686E-01	4.4841E-01	4.4995E-01	4.5150E-01
80	4.5304E-01	4.5458E-01	4.5612E-01	4.5766E-01	4.5921E-01	4.6075E-01	4.6229E-01	4.6383E-01	4.6537E-01	4.6691E-01
	4.6845E-01	4.6998E-01	4.7152E-01	4.7306E-01	4.7460E-01	4.7613E-01	4.7767E-01	4.7921E-01	4.8074E-01	4.8228E-01

Table II R values for $Fe_{32}Ni_{36}Cr_{14}P_{12}B_6$

ΔE =	1	2	3	4	5	6	7	8	9	10
0	1,6229-03	3,2472-	4,8[illegible]4-03	6,4072-03	8,1157-03	9,7379-03	1,1360-02	1,2901-02	1.4402-02	1.6223-02
	1,7[illegible]	1,9466-02	4,1[illegible]4-02	[illegible]	2,4323-02	2,5963-02	2,7563-02	2,9178-02	3,0796-02	3.2414-02
20	[illegible]	[illegible],5462-	3,7265-02	[illegible]	4,0497-02	4,2113-02	4,3729-02	4,5344-02	4.6958-02	4.8573-02
	[illegible]	[illegible]	3,9414-02	[illegible]	5,6044-02	5,8253-02	5,9863-02	6,1477-02	6,3088-02	6.4700-02
40	[illegible]	6,7921-	4,6572-02	7,1142-02	7,2731-02	7,4361-02	7,5970-02	7,7578-02	7,9187-02	8.0795-02
	[illegible]	[illegible]	8,4617-02	8,7224-02	8,8831-02	9,0437-02	9,2043-02	9.3649-02	9.5254-02	9.6859-02
60	[illegible]	1,3002-01	1,0167-01	[illegible]	1,0488-01	1,0649-01	1,0809-01	1,0969-01	1.1129-01	1.1289-01
	[illegible]	1,2619-01	4,1770-01	1,2073-01	1,2090-01	1,2250-01	1,2410-01	1,2570-01	1.2729-01	1.2889-01
80	[illegible]	1,3209-01	4,5769-01	1,7529-01	1,3688-01	1.3848-01	1,4008-01	1,4167-01	1,4327-01	1.4487-01
	[illegible]	1,4800-01	4,4965-01	1,5229-01	1,5284-01	1,5443-01	1,5603-01	1,5762-01	1,5921-01	1.6081-01
100	[illegible]	1,6355-01	4,6558-01	1,6717-01	1,6877-01	1,7036-01	1,7195-01	1,7354-01	1,7513-01	1.7672-01
	1,7921-01	1,7990-01	4,8149-01	1,8227-01	1,8466-01	1,8625-01	1,8784-01	1,8943-01	1,9101-01	1.9260-01
20	1,9419-01	1,9577-01	4,0736-01	1,5994-01	2,0053-01	2,0211-01	2,0370-01	2,0540-01	2,0687-01	2.0845-01
	[illegible]	2,1162-01	2,1326-01	2,1479-01	2,1637-01	2,1795-01	2,1953-01	2,2111-01	2,2269-01	2.2428-01
40	[illegible]	2,2746-01	2,2932-01	2,7082-01	2,3218-01	2,3374-01	2,3534-01	2,3691-01	2,3849-01	2.4007-01
	2,4189-01	2,4323-01	4,1486-01	2,4678-01	2,4796-01	2,4953-01	2,5111-01	2,5269-01	2,5426-01	2.5584-01
60	2,5741-01	2,5699-01	4,6356-01	2,4724-01	2,6371-01	2,6529-01	2,6686-01	2,6843-01	2,7000-01	2.7158-01
	2,7913-01	2,7472-01	4,9420-01	2,7768-01	2,7943-01	2,8100-01	2,8258-01	2,8415-01	2,8572-01	2.8729-01
80	2,9086-01	2,9243-01	4,0240-01	2,9376-01	2,9513-01	2,9670-01	2,9827-01	2,9984-01	3,0140-01	3.0297-01
	3,0494-01	3,0481-01	3,0767-01	3,0974-01	3,1080-01	3,1237-01	3,1393-01	3,1550-01	3,1706-01	3.1863-01
200	3,2019-01	3,2172-01	3,2332-01	3,2489-01	3,2645-01	3,2801-01	3,2957-01	3,3114-01	3,3270-01	3.3426-01
	[illegible]	3,3734-01	4,9774-01	3,4076-01	3,4207-01	3,4363-01	3,4519-01	3,4675-01	3,4831-01	3.4986-01
20	3,5142-01	3,5298-01	[illegible]	3,5618-01	3,5766-01	3,5922-01	3,6077-01	3,6233-01	3,6389-01	3.6544-01
	[illegible]	3,6856-01	[illegible]	3,7247-01	3,7322-01	3,7478-01	3,7633-01	3,7789-01	3,7944-01	3.8100-01
40	3,8259-01	3,8411-01	3,8586-01	[illegible]	3,8877-01	3,9032-01	3,9187-01	3,9344-01	3,9499-01	3.9653-01
	[illegible]	3,9963-01	4,0118-01	4,0273-01	4,0428-01	4,0583-01	4,0738-01	4,0893-01	4,1048-01	4.1203-01
60	[illegible]	4,1517-01	[illegible]	[illegible]	4,1978-01	4,2132-01	4,2287-01	4,2442-01	4,2597-01	4.2751-01
	4,2906-01	4,3261-01	[illegible]	[illegible]	4,3525-01	4,3679-01	4,3834-01	4,3989-01	4,4143-01	4.4297-01
80	4,4652-01	[illegible]	[illegible]	[illegible]	4,5069-01	4,5224-01	4,5378-01	4,5532-01	4,5687-01	4.5841-01
	4,5935-01	[illegible]	[illegible]	[illegible]	4,6612-01	4,6766-01	4,6920-01	4,7074-01	4,7228-01	4.7382-01

Table III R values for $Fe_{40}Ni_{40}B_{20}$

ΔE =	1	2	3	4	5	6	7	8	9	10
0	1.6630-03	3.1097-03	4.7001-03	6.3937-03	7.9970-03	9.5956-03	1.1194-02	1.2710-02	1.4300-02	1.5987-02
	1.7504-02	1.9181-02	2.0778-02	2.2377-02	2.3970-02	2.5566-02	2.7161-02	2.8756-02	3.0351-02	3.1946-02
20	3.3536-02	3.5134-02	3.6728-02	3.8327-02	3.9915-02	4.1530-02	4.3101-02	4.4693-02	4.6285-02	4.7877-02
	4.9464-02	5.1069-02	5.2661-02	5.4249-02	5.5838-02	5.7423-02	5.9012-02	6.0602-02	6.2191-02	6.3781-02
40	6.5369-02	6.6958-02	6.8546-02	7.0135-02	7.1720-02	7.3310-02	7.4900-02	7.6484-02	7.8070-02	7.9657-02
	8.1243-02	8.2829-02	8.4414-02	8.5994-02	8.7584-02	8.9169-02	9.0754-02	9.2338-02	9.3922-02	9.5506-02
60	9.7089-02	9.8672-02	1.0025-01	1.0183-01	1.0342-01	1.0501-01	1.0656-01	1.0817-01	1.0975-01	1.1133-01
	1.1291-01	1.1449-01	1.1607-01	1.1764-01	1.1923-01	1.2081-01	1.2238-01	1.2397-01	1.2554-01	1.2712-01
80	1.2870-01	1.3029-01	1.3186-01	1.3344-01	1.3501-01	1.3659-01	1.3816-01	1.3974-01	1.4132-01	1.4289-01
	1.4447-01	1.4604-01	1.4762-01	1.4919-01	1.5077-01	1.5234-01	1.5391-01	1.5549-01	1.5706-01	1.5863-01
100	1.6021-01	1.6178-01	1.6335-01	1.6493-01	1.6650-01	1.6807-01	1.6964-01	1.7121-01	1.7278-01	1.7435-01
	1.7592-01	1.7749-01	1.7906-01	1.8063-01	1.8220-01	1.8377-01	1.8534-01	1.8691-01	1.8847-01	1.9004-01
20	1.9161-01	1.9318-01	1.9474-01	1.9631-01	1.9788-01	1.9944-01	2.0101-01	2.0258-01	2.0414-01	2.0571-01
	2.0727-01	2.0884-01	2.1040-01	2.1197-01	2.1353-01	2.1509-01	2.1666-01	2.1822-01	2.1978-01	2.2135-01
40	2.2291-01	2.2447-01	2.2603-01	2.2760-01	2.2916-01	2.3072-01	2.3228-01	2.3384-01	2.3540-01	2.3696-01
	2.3852-01	2.4008-01	2.4164-01	2.4320-01	2.4476-01	2.4632-01	2.4788-01	2.4944-01	2.5099-01	2.5255-01
60	2.5411-01	2.5567-01	2.5723-01	2.5879-01	2.6034-01	2.6191-01	2.6345-01	2.6501-01	2.6656-01	2.6812-01
	2.6967-01	2.7123-01	2.7279-01	2.7434-01	2.7589-01	2.7745-01	2.7900-01	2.8056-01	2.8211-01	2.8366-01
80	2.8522-01	2.8677-01	2.8832-01	2.8988-01	2.9143-01	2.9298-01	2.9453-01	2.9608-01	2.9763-01	2.9918-01
	3.0073-01	3.0228-01	3.0383-01	3.0538-01	3.0693-01	3.0848-01	3.1003-01	3.1158-01	3.1313-01	3.1468-01
200	3.1623-01	3.1777-01	3.1932-01	3.2087-01	3.2242-01	3.2396-01	3.2551-01	3.2706-01	3.2860-01	3.3015-01
	3.3170-01	3.3324-01	3.3479-01	3.3633-01	3.3788-01	3.3942-01	3.4096-01	3.4251-01	3.4406-01	3.4560-01
20	3.4715-01	3.4869-01	3.5023-01	3.5177-01	3.5332-01	3.5485-01	3.5640-01	3.5795-01	3.5949-01	3.6103-01
	3.6257-01	3.6411-01	3.6566-01	3.6720-01	3.6874-01	3.7028-01	3.7182-01	3.7336-01	3.7490-01	3.7644-01
40	3.7798-01	3.7952-01	3.8106-01	3.8260-01	3.8413-01	3.8567-01	3.8721-01	3.8875-01	3.9029-01	3.9182-01
	3.9336-01	3.9490-01	3.9644-01	3.9797-01	3.9951-01	4.0105-01	4.0259-01	4.0413-01	4.0565-01	4.0719-01
60	4.0872-01	4.1026-01	4.1179-01	4.1333-01	4.1486-01	4.1641-01	4.1793-01	4.1947-01	4.2100-01	4.2253-01
	4.2407-01	4.2560-01	4.2713-01	4.2867-01	4.3020-01	4.3173-01	4.3326-01	4.3480-01	4.3633-01	4.3786-01
80	4.3939-01	4.4092-01	4.4245-01	4.4398-01	4.4551-01	4.4704-01	4.4857-01	4.5011-01	4.5163-01	4.5316-01
	4.5469-01	4.5622-01	4.5775-01	4.5927-01	4.6081-01	4.6234-01	4.6387-01	4.6539-01	4.6692-01	4.6845-01

Table IV R values for $Fe_{80}B_{20}$

ΔE =	1	2	3	4	5	6	7	8	9	10
0	1.0376-03	3.2769-03	6.9117-03	0.9481-03	0.1841-03	9.8197-03	1.1435-02	1.3090-02	1.4726-02	1.6396-02
	1.7992-02	1.9645-02	2.1258-02	2.2893-02	2.4522-02	2.6133-02	2.7789-02	2.9419-02	3.1046-02	3.2676-02
20	3.4309-02	3.5934-02	3.7563-02	3.9192-02	4.0820-02	4.2447-02	4.4074-02	4.5701-02	4.7327-02	4.8953-02
	5.0579-02	5.2204-02	5.3829-02	5.5453-02	5.7077-02	5.8701-02	6.0324-02	6.1947-02	6.3569-02	6.5191-02
40	6.6813-02	6.8434-02	7.0055-02	7.1675-02	7.3295-02	7.4915-02	7.6534-02	7.8153-02	7.9771-02	8.1389-02
	8.3007-02	8.4624-02	8.6241-02	8.7857-02	8.9473-02	9.1089-02	9.2704-02	9.4319-02	9.5934-02	9.7548-02
60	9.9162-02	1.0078-01	1.0239-01	1.0400-01	1.0561-01	1.0722-01	1.0884-01	1.1045-01	1.1206-01	1.1367-01
	1.1528-01	1.1689-01	1.1850-01	1.2010-01	1.2171-01	1.2332-01	1.2493-01	1.2654-01	1.2814-01	1.2975-01
80	1.3135-01	1.3296-01	1.3457-01	1.3617-01	1.3777-01	1.3938-01	1.4098-01	1.4259-01	1.4419-01	1.4579-01
	1.4739-01	1.4900-01	1.5060-01	1.5220-01	1.5380-01	1.5540-01	1.5700-01	1.5860-01	1.6020-01	1.6180-01
100	1.6339-01	1.6499-01	1.6659-01	1.6819-01	1.6978-01	1.7138-01	1.7298-01	1.7457-01	1.7617-01	1.7776-01
	1.7936-01	1.8095-01	1.8255-01	1.8414-01	1.8573-01	1.8733-01	1.8892-01	1.9051-01	1.9210-01	1.9369-01
20	1.9528-01	1.9687-01	1.9846-01	2.0005-01	2.0164-01	2.0323-01	2.0482-01	2.0641-01	2.0800-01	2.0959-01
	2.1117-01	2.1276-01	2.1434-01	2.1593-01	2.1752-01	2.1910-01	2.2069-01	2.2227-01	2.2386-01	2.2544-01
40	2.2702-01	2.2861-01	2.3019-01	2.3177-01	2.3336-01	2.3494-01	2.3652-01	2.3810-01	2.3968-01	2.4126-01
	2.4284-01	2.4442-01	2.4600-01	2.4758-01	2.4916-01	2.5074-01	2.5231-01	2.5389-01	2.5547-01	2.5704-01
60	2.5862-01	2.6020-01	2.6177-01	2.6335-01	2.6492-01	2.6650-01	2.6807-01	2.6965-01	2.7122-01	2.7279-01
	2.7437-01	2.7594-01	2.7751-01	2.7908-01	2.8065-01	2.8222-01	2.8380-01	2.8537-01	2.8694-01	2.8851-01
80	2.9008-01	2.9164-01	2.9321-01	2.9478-01	2.9635-01	2.9792-01	2.9948-01	3.0105-01	3.0262-01	3.0418-01
	3.0575-01	3.0732-01	3.0888-01	3.1045-01	3.1201-01	3.1357-01	3.1514-01	3.1670-01	3.1827-01	3.1983-01
200	3.2139-01	3.2295-01	3.2451-01	3.2608-01	3.2764-01	3.2920-01	3.3076-01	3.3232-01	3.3388-01	3.3544-01
	3.3700-01	3.3856-01	3.4012-01	3.4167-01	3.4323-01	3.4479-01	3.4635-01	3.4790-01	3.4946-01	3.5102-01
20	3.5257-01	3.5413-01	3.5568-01	3.5724-01	3.5879-01	3.6035-01	3.6190-01	3.6345-01	3.6501-01	3.6656-01
	3.6811-01	3.6966-01	3.7122-01	3.7277-01	3.7432-01	3.7587-01	3.7742-01	3.7897-01	3.8052-01	3.8207-01
40	3.8362-01	3.8517-01	3.8672-01	3.8827-01	3.8982-01	3.9136-01	3.9291-01	3.9446-01	3.9600-01	3.9755-01
	3.9910-01	4.0064-01	4.0219-01	4.0373-01	4.0528-01	4.0682-01	4.0837-01	4.0991-01	4.1146-01	4.1300-01
60	4.1454-01	4.1609-01	4.1763-01	4.1917-01	4.2071-01	4.2225-01	4.2379-01	4.2534-01	4.2688-01	4.2842-01
	4.2996-01	4.3150-01	4.3304-01	4.3458-01	4.3611-01	4.3765-01	4.3919-01	4.4073-01	4.4227-01	4.4380-01
80	4.4534-01	4.4688-01	4.4841-01	4.4995-01	4.5149-01	4.5302-01	4.5456-01	4.5609-01	4.5763-01	4.5916-01
	4.6069-01	4.6243-01	4.6376-01	4.6530-01	4.6683-01	4.6836-01	4.6989-01	4.7143-01	4.7296-01	4.7449-01

Table V R values for $Fe_{83}B_{17}$

ΔE =	1	2	3	4	5	6	7	8	9	10
0	1.6198-03	3.2271-03	4.8401-03	6.4546-03	8.0648-03	9.6765-03	1.1288-02	1.2899-02	1.4509-02	1.6120-02
	1.7729-02	1.9339-02	2.0948-02	2.2558-02	2.4165-02	2.5772-02	2.7380-02	2.8987-02	3.0593-02	3.2200-02
20	3.3806-02	3.5411-02	3.7016-02	3.8621-02	4.0225-02	4.1829-02	4.3432-02	4.5035-02	4.6638-02	4.8240-02
	4.9842-02	5.1444-02	5.3045-02	5.4646-02	5.6246-02	5.7846-02	5.9445-02	6.1043-02	6.2643-02	6.4242-02
40	6.5840-02	6.7437-02	6.9035-02	7.0632-02	7.2228-02	7.3824-02	7.5420-02	7.7015-02	7.8610-02	8.0205-02
	8.1799-02	8.3392-02	8.4986-02	8.6579-02	8.8171-02	8.9764-02	9.1356-02	9.2947-02	9.4538-02	9.6129-02
60	9.7719-02	9.9309-02	1.0089-01	1.0249-01	1.0408-01	1.0566-01	1.0725-01	1.0884-01	1.1043-01	1.1201-01
	1.1360-01	1.1519-01	1.1677-01	1.1836-01	1.1994-01	1.2153-01	1.2311-01	1.2470-01	1.2628-01	1.2786-01
80	1.2945-01	1.3103-01	1.3261-01	1.3419-01	1.3577-01	1.3735-01	1.3893-01	1.4051-01	1.4209-01	1.4367-01
	1.4525-01	1.4683-01	1.4841-01	1.4999-01	1.5156-01	1.5314-01	1.5472-01	1.5629-01	1.5787-01	1.5945-01
100	1.6102-01	1.6260-01	1.6417-01	1.6575-01	1.6732-01	1.6889-01	1.7047-01	1.7204-01	1.7361-01	1.7518-01
	1.7675-01	1.7833-01	1.7990-01	1.8147-01	1.8304-01	1.8461-01	1.8618-01	1.8776-01	1.8931-01	1.9088-01
20	1.9245-01	1.9402-01	1.9558-01	1.9715-01	1.9872-01	2.0028-01	2.0185-01	2.0342-01	2.0498-01	2.0655-01
	2.0811-01	2.0967-01	2.1124-01	2.1280-01	2.1436-01	2.1593-01	2.1749-01	2.1905-01	2.2061-01	2.2217-01
40	2.2373-01	2.2529-01	2.2685-01	2.2841-01	2.2997-01	2.3153-01	2.3309-01	2.3465-01	2.3621-01	2.3776-01
	2.3932-01	2.4088-01	2.4243-01	2.4399-01	2.4555-01	2.4710-01	2.4866-01	2.5021-01	2.5177-01	2.5332-01
60	2.5487-01	2.5643-01	2.5798-01	2.5953-01	2.6109-01	2.6264-01	2.6419-01	2.6574-01	2.6729-01	2.6884-01
	2.7039-01	2.7194-01	2.7349-01	2.7504-01	2.7659-01	2.7814-01	2.7969-01	2.8123-01	2.8278-01	2.8433-01
80	2.8588-01	2.8742-01	2.8897-01	2.9051-01	2.9206-01	2.9361-01	2.9515-01	2.9669-01	2.9824-01	2.9978-01
	3.0133-01	3.0287-01	3.0441-01	3.0595-01	3.0750-01	3.0904-01	3.1058-01	3.1212-01	3.1366-01	3.1520-01
200	3.1674-01	3.1828-01	3.1982-01	3.2136-01	3.2290-01	3.2444-01	3.2598-01	3.2751-01	3.2903-01	3.3059-01
	3.3213-01	3.3366-01	3.3520-01	3.3674-01	3.3827-01	3.3981-01	3.4134-01	3.4288-01	3.4441-01	3.4594-01
20	3.4748-01	3.4901-01	3.5054-01	3.5208-01	3.5361-01	3.5514-01	3.5667-01	3.5820-01	3.5973-01	3.6127-01
	3.6280-01	3.6433-01	3.6586-01	3.6739-01	3.6891-01	3.7044-01	3.7197-01	3.7350-01	3.7503-01	3.7656-01
40	3.7808-01	3.7961-01	3.8114-01	3.8266-01	3.8419-01	3.8571-01	3.8724-01	3.8876-01	3.9029-01	3.9181-01
	3.9334-01	3.9486-01	3.9639-01	3.9791-01	3.9943-01	4.0095-01	4.0248-01	4.0400-01	4.0552-01	4.0704-01
60	4.0856-01	4.1008-01	4.1160-01	4.1313-01	4.1464-01	4.1616-01	4.1768-01	4.1920-01	4.2072-01	4.2224-01
	4.2376-01	4.2528-01	4.2679-01	4.2831-01	4.2983-01	4.3134-01	4.3286-01	4.3438-01	4.3589-01	4.3741-01
80	4.3892-01	4.4044-01	4.4195-01	4.4347-01	4.4498-01	4.4649-01	4.4801-01	4.4952-01	4.5103-01	4.5255-01
	4.5406-01	4.5557-01	4.5708-01	4.5859-01	4.6011-01	4.6162-01	4.6313-01	4.6464-01	4.6615-01	4.6766-01

Table VI R values for Si_{100}

ΔE =	1	2	3	4	5	6	7	8	9	10
0	3.[illegible]-03	6.9217-03	1.[illegible]	1.3839-02	1.7296-02	2.0752-02	2.4209-02	2.7662-02	3.1112-02	3.4566-02
	3.[illegible]-02	[illegible]	[illegible]	4.8338-02	5.1804-02	5.5268-02	5.8692-02	6.2134-02	6.5576-02	6.9016-02
20	[illegible]	[illegible]5893-02	7.[illegible]	8.2756-02	8.6201-02	8.9634-02	9.3067-02	9.6498-02	9.9928-02	1.0330-01
	1.0[illegible]-01	1.1021-01	1.1364-01	1.1706-01	1.2049-01	1.2391-01	1.2733-01	1.3075-01	1.3417-01	1.3759-01
40	1.[illegible]-01	1.4462-01	1.4784-01	1.5125-01	1.5466-01	1.5807-01	1.6148-01	1.6489-01	1.6830-01	1.7171-01
	1.[illegible]-01	1.7852-01	1.8192-01	1.8533-01	1.8873-01	1.9213-01	1.9553-01	1.9893-01	2.0232-01	2.0572-01
60	2.[illegible]	2.1251-01	2.[illegible]590-01	2.1929-01	2.2268-01	2.2607-01	2.2946-01	2.3285-01	2.3623-01	2.3962-01
	2.[illegible]-01	2.4638-01	2.4977-01	2.5315-01	2.5653-01	2.5991-01	2.6329-01	2.6666-01	2.7[illegible]-01	2.7341-01
80	2.7[illegible]8-01	2.8016-01	2.8353-01	2.8690-01	2.9027-01	2.9363-01	2.9700-01	3.0037-01	3.0373-01	3.0710-01
	3.[illegible]-01	3.1382-01	3.[illegible]718-01	3.2054-01	3.2390-01	3.2725-01	3.3061-01	3.3396-01	3.3732-01	3.4067-01
100	[illegible]	3.[illegible]	3.[illegible]072-01	3.5407-01	3.5742-01	3.6076-01	3.6411-01	3.6745-01	3.7081-01	3.7416-01
	3.[illegible]	3.8082-01	3.[illegible]	3.8750-01	3.9083-01	3.9417-01	3.9750-01	4.0084-01	4.0417-01	4.0750-01
20	4.[illegible]	[illegible]	4.1749-01	4.2081-01	4.2414-01	4.2747-01	4.3079-01	4.3411-01	4.3743-01	4.4075-01
	[illegible]	4.4[illegible]73-01	4.5071-01	4.5403-01	4.5734-01	4.6066-01	4.6397-01	4.6728-01	4.7059-01	4.7390-01
40	4.[illegible]-01	4.8051-01	4.8383-01	4.8713-01	4.9044-01	4.9374-01	4.9705-01	5.0035-01	5.0365-01	5.[illegible]695-01
	5.[illegible]-01	5.[illegible]	5.[illegible]684-01	5.2014-01	5.2343-01	5.2672-01	5.3002-01	5.3331-01	5.3660-01	5.3989-01
60	5.[illegible]-01	5.4646-01	5.4975-01	5.5303-01	5.5632-01	5.5960-01	5.6288-01	5.6616-01	5.6944-01	5.7272-01
	5.[illegible]-01	5.7[illegible]-01	5.8255-01	5.8583-01	5.8910-01	5.9237-01	5.9564-01	5.9891-01	6.0218-01	6.0545-01
80	6.[illegible]2-01	6.1199-01	6.[illegible]525-01	6.1852-01	6.2178-01	6.2506-01	6.2830-01	6.3156-01	6.3482-01	6.3808-01
	6.[illegible]-01	6.4459-01	6.[illegible]785-01	6.5110-01	6.5434-01	6.5761-01	6.6086-01	6.6411-01	6.6736-01	6.7061-01
200	6.[illegible]385-01	6.7710-01	6.[illegible]034-01	6.8359-01	6.8683-01	6.9007-01	6.9331-01	6.9655-01	6.9979-01	7.0303-01
	7.[illegible]-01	7.0951-01	7.[illegible]274-01	7.1597-01	7.1921-01	7.2244-01	7.2567-01	7.2890-01	7.3213-01	7.3536-01
20	7.[illegible]-01	7.4181-01	7.[illegible]503-01	7.4826-01	7.5148-01	7.5470-01	7.5792-01	7.6114-01	7.6436-01	7.6758-01
	7.[illegible]-01	7.[illegible]401-01	7.[illegible]723-01	7.8044-01	7.8365-01	7.8687-01	7.9008-01	7.9329-01	7.9650-01	7.9970-01
40	8.0291-01	8.0612-01	8.[illegible]932-01	8.1253-01	8.1573-01	8.1893-01	8.2213-01	8.2533-01	8.2853-01	8.3173-01
	8.[illegible]493-01	8.3812-01	8.[illegible]132-01	8.4451-01	8.4770-01	8.5090-01	8.5409-01	8.5728-01	8.6047-01	8.6366-01
60	8.[illegible]684-01	8.7003-01	8.[illegible]322-01	8.7640-01	8.7958-01	8.8277-01	8.8595-01	8.8913-01	8.9231-01	8.9549-01
	8.[illegible]-01	9.0184-01	9.[illegible]502-01	9.0819-01	9.1137-01	9.1456-01	9.1771-01	9.2088-01	9.2405-01	9.2722-01
80	9.3039-01	9.3355-01	9.[illegible]672-01	9.3989-01	9.4305-01	9.4622-01	9.4938-01	9.5254-01	9.5570-01	9.5886-01
	9.[illegible]2-01	9.6[illegible]	9.[illegible]837-01	9.[illegible]149-01	9.7466-01	9.7780-01	9.8095-01	9.8410-01	9.8725-01	9.9040-01

APPENDIX

CODE FOR DECONVOLUTING ALPHA-SPECTRA USING FOURIER TRANSFORMATION

In *Figs. 1, 2* and *3* a mathematical technique called DECONVOLUTION was used to calculate the smoothed concentration distribution. This technique subtracts the line broadening contribution of the detector system from the measured spectrum and enables the depth resolution to be improved by some 10 %. The depth resolution in our cases was better than $\pm$ 40 nm, after deconvolution.

The advantage of the deconvolution technique over other techniques is that it can automatically be employed in practice for a wide variety of spectral forms, without the need for any preliminary assumption.

In the FORTRAN program the following mathematical treatment was used for the deconvolution of alpha-spectra:
The measured amplitude spectrum is approximated with its Fourier series for N=64, 128, 256 or 512 equidistant discrete spectral values

$$y(x) = \sum_{k=0}^{N-1} c_k e^{ikx} \qquad (A_1)$$

where c_k Fourier coefficients are calculated by fast Fourier transform /FFT/.

Let us consider for the Fourier transformation that the investigated part of the spectrum /from k=0 to k=N/ is the basic period of an infinite periodic function. This function, however, has generally large abrupt junctions at the boundaries because of the background structure and these lead to an additional noise contribution to the Fourier spectrum. To avoid this, Lánczos [6] proposed the subtraction of a saw-tooth base line from Eg.(A_1) which makes the function values zero at both ends of the spectrum. Therefore, the periodic function will be "continuous" apart from statistical fluctuations and we can get rid of a long tail in the Fourier spectrum decreasing with 1/k.

Naturally this step is advantageous but from the physical point of view it is necessary to subtract the real background. The quadratic polynomial is a more realistic background in the cases of alpha-spectra. First, therefore, we subtract a quadratic background which removes a contribution from the Fourier spectrum decreasing proportionally to $1/k^2$ and we subsequently subtract a saw-tooth base line from the rest. Assumming that the deconvolution does not effect the latter component, it is restored to the deconvoluted distribution.

The same procedure was extended to the R/x/ resolution function which can be obtained as a response spectrum for a boron momolayer /δ-function/, recorded under similar conditions to those in which the measurements were carried out.

The data of the Fourier coefficients are divided by their respective resolution coefficients and we make the inverse transform of this final expansion.

Although the mathematical steps are straighforward, the use of these steps in practice lead to oscillation and distortion of actual experimental data. Namely, the Fourier coefficients of a regular smooth functions usually decrease very rapidly /with $1/k^3$/ and after a characteristic part, usually in the last two-thirds of the spectrum, turn into random fluctuation due to the statistical nature of the experimental data points. In this high frequency region the coefficients fluctuate like noise about some small mean value and the ratio of the spectrum and the response coefficient may have randomly great values and we obtain violent oscillations.

Figures 5a,b and *6a,b* show the calculated c_k Fourier coefficients /real part/ for two different alpha-spectra as a function of the k index. It can be seen from these figures that it is necessary to truncate the Fourier expansion at the high-frequency components so as to avoid the subsequent oscillation. At the same time care should be taken not to throw away the characteristic part of the Fourier spectrum, i.e. the oversmoothing of the spectrum should be avoided. Also, the sharp cut-off leads to Gibbs oscillation. Following the suggestion of Lánczos [6], the σ-factor can minimize this type of oscillation.

The difficulties that arise explain why the application of the method does not come into general use. In this paper we describe how these results may be applied on alpha-spectra. The procedure for the automatic determination of the cut-off frequency is as follows:

Let the cut-off frequency be at the M^{th} index, where

$$c_M \approx M \cdot \varepsilon \quad , \qquad (A_2)$$

where ε is the noise. We consider from Eq.(A_1) the truncated part of the spectrum constructed from the first /M-1/ components

$$y(x) = \sum_{k=0}^{M-1} c_k e^{ikx} \qquad (A_3)$$

The functions (A_1) and (A_3) differ from each other and the fitting accuracy of the two functions /S^2/ can be calculated from the "distance" of the two functions:

$$S^2 = \sum_{x=1}^{N} \frac{(y(x)-Y(x))^2}{N-1} \quad . \qquad (A_4)$$

According to Lánczos [6], Eq.(A_4) may be replaced by

$$S^2 = \frac{1}{2} \sum_{j=k+1}^{N-3} c_j^2 \quad , \qquad (A_5)$$

that is, the variance of using only the first M coefficients is equal to one-half the sum of the squares of the rejected forms. Equation (A_5) is a more simple expression for the accuracy of the fit, but a conceptual evaluation is needed which indicates how good the fit should be. As is known, this evaluation is performed by the error integral. In general it would be obvious to

expect normal distribution for data points. However, experience shows that the degrees of freedom are small for the truncated expansion. The cut-off frequency in our case is generally not higher than M=5-25 indexes. It is, therefore, advisable to evaluate the error by means of the STUDENT cumulative distribution function. The STUDENT distribution can be defined as a confidence level for the error rate to be expected as the deviation of the Y/x/ approximating function. Thus we can calculate a "figure of merit" when we consider the increasing number of coefficients.

$$\text{merit}(k) = T(M)\sqrt{\frac{S^2}{M}} \quad , \qquad (A_6)$$

where M=/N-1/-k-1, T is the STUDENT table corresponding to the desired confidence level, M and S are the quantities defined in Eq.(A_5).

As can be seen in *Fig. 5a,b* Eq.(A_6) usually has a distinct minimum except when the data points had poor statistics */Fig. 6a,b/*. This minimum will occur for a value of k where additional coefficients cause more noise than fitting accuracy.

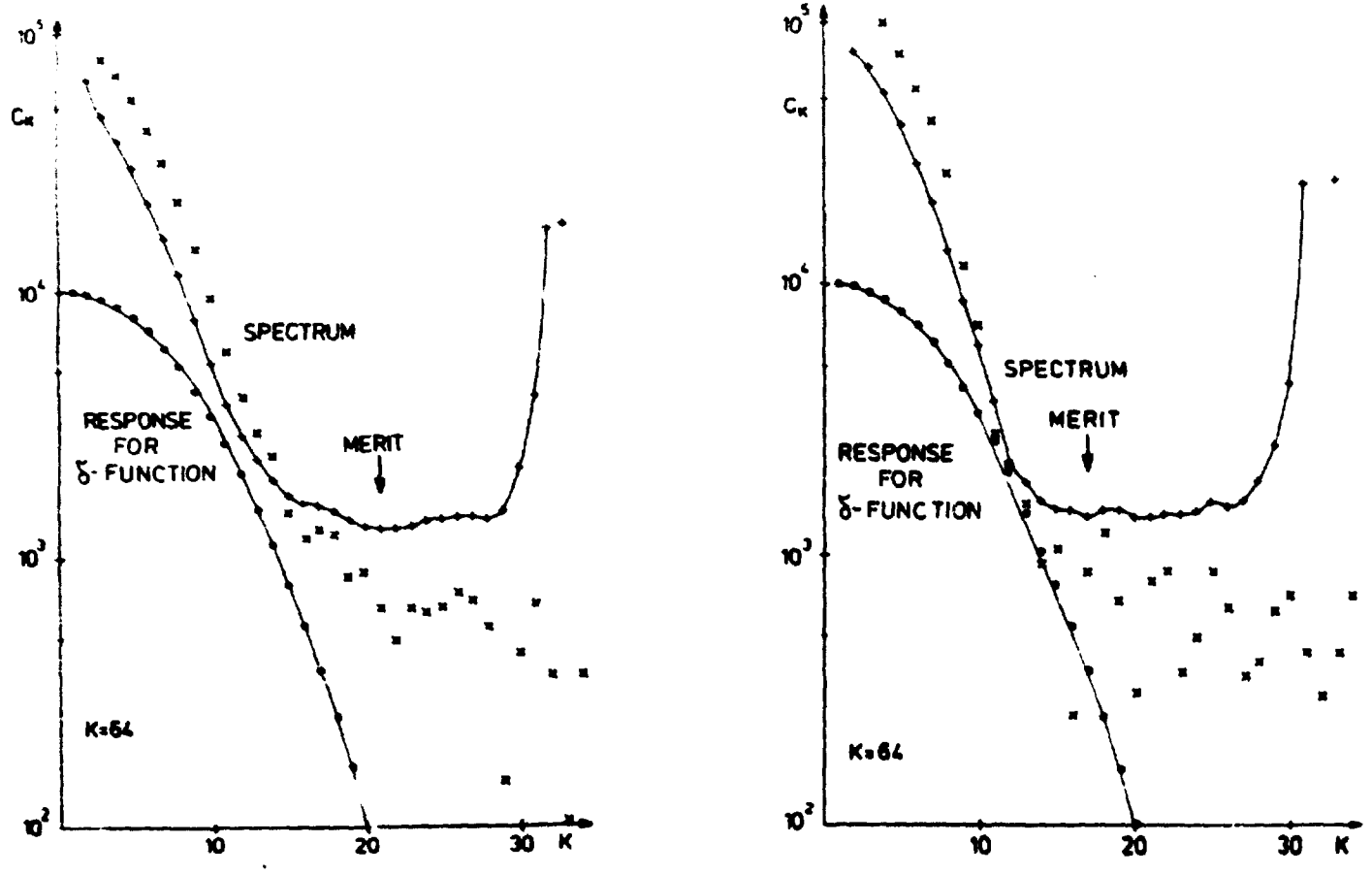

Fig. 5/a, b

Fourier coefficient values versus the number of coefficients for the case when the experimental data points had good statistics

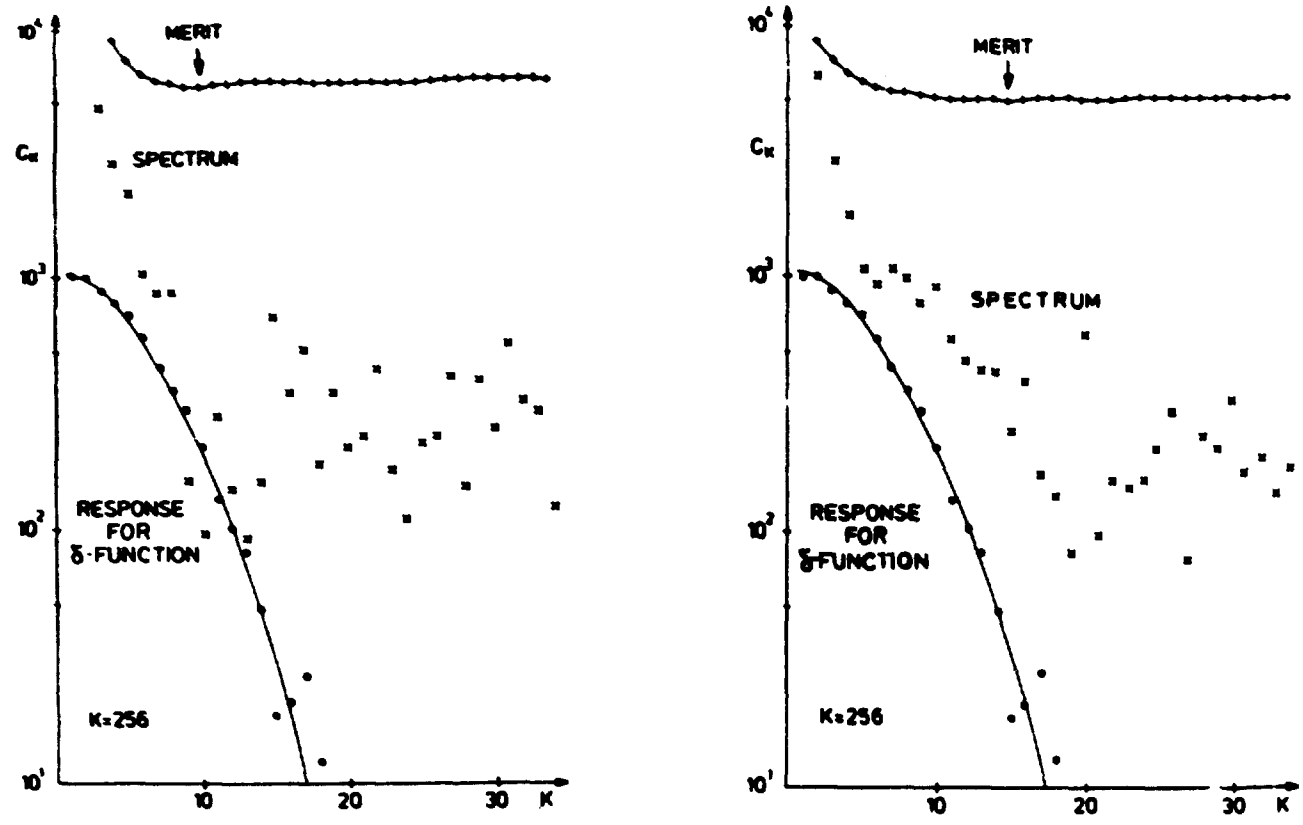

Fig. 6/a, b

Fourier coefficient values versus the number of coefficients for the case when the experimental data points had poor statistics

```
      PROGRAM DECONV
C
C FORTRAN PROGRAM FOR DECONVOLUTION OF ALPHA AMPLITUDE SPECTRA
C MEASURED IN B10(N,ALPHA)LI7 REACTION ON ION-IMPLANTED SILICON
C
      COMPLEX BS,DC,DD
      COMPLEX FI, FIC
      DIMENSION BS(256),DD(256),BD(256),V(256)
      DIMENSION IS(256),S(256)
      COMMON II,IS,S,NE
      COMMON /CAL/A,B,E1,E2,E3,P0,P1,P2,P3
      COMMON /CONST/W1,W2,W3,RA,RB,DA,DB,AREA,MON,TN,NN,MONR,JL,IFLAG
      COMMON /CNST1/DC,DC,IBL1,IBL2,IBR1,IBR2,NCH,ICUT,II1
      COMMON /TEXT/ IC(72),IC5(72),I2,I1R,I2R
      COMMON /ST/TTBB(30)
      DATA PI/3.14159/
      DATA IBL,IAST/1H ,1H*/
C
1001  FORMAT(6F6.3)
1002  FORMAT(2I4)
1003  FORMAT(3F8.2)
1004  FORMAT(F8.4)
1005  FORMAT(1H1,30X,'RESPONSE SPECTRUM'//10X,72A1)
1006  FORMAT(6X,23HRESPONSE PEAK POSITION:,F8.2)
1007  FORMAT(/11X,21HFOURIER COEFFICIENTS://2X,10K,16X,
     18HSPECTRUM,20X,8HRESPONSE,26X,13HDECONVOLUTION,15X,5HCRIT)
1008  FORMAT(1X,I4,3E12.3,3E12.6,4E12.3)
1009  FORMAT(1X,I4,3E12.3)
1010  FORMAT(1X,22HBACKGROUND PARAMETERS:,F8.4,2F8.2)
1011  FORMAT(/2X,10K,9X,22HSMOOTHED DECONVOLUTION)
1016  FORMAT(/8H CHANNEL,4X,6HENERGY,2X,8HMEASURED,2X,12HDECONVOLUTED,
     19X,5HDEPTH,6X,13HCONCENTRATION/40X,7H MICRON,7X,13HN/CM3*10**-17)
1017  FORMAT(1X,I5,F12.4,2E11.1,E16.4,F16.1)
1018  FORMAT(32H INTEGRATED QUANTITY OF B ATOMS:,E10.4,7H*10**17)
C
C **** SET CONSTANTS
C
C LAYER THICKNESS COEFFICIENT (IN MICRON) FOR ENERGY LOSS (MEV) OF
C       ALPHA PARTICLES IN RANDOM SILICON
      DXDE=3.46
C CONSTANTS REFERRING TO THE RESPONSE SPECTRUM
C PEAK ENERGY IN MEV
2     E1=1.471
3     E2=2.050
4     E3=2.730
C RELIABILITY WEIGHTS FOR THE ENERGY CALIBRATION
5     W1=1.
6     W2=0.2
7     W3=0.5
C
C **** INPUT CONSTANTS
C
C READ STUDENT T TABLE
C DEGREES OF FREEDOM I=1,30        PROBABILITY  0.01
8     READ 1001,(TTBB(I),I=1,30)
C READ CONSTANTS REFERRING TO THE RESPONSE SPECTRUM:
C READ LENGTH TO BE DECONVOLUTED AND SEARCHING LIMIT
9     READ 1002,N,NE
10    N=ALOG(FLOAT(N))/ALOG(2.)+0.00001
C READ PEAK POSITIONS (AS ABOVE)
11    READ 1003,P1,P2,P3
C READ ENERGY CORRECTIONS
12    READ 1003,DE1,DE2,DE3
```

```
      F1=E1-BE1
      F2=E2-BE2
      F3=E3-BE3
C READ NUMBER OF IMPLANTED B ATOMS IN RESPONSE SAMPLE IN 10**17 UNITS
      READ 1004,TN
C READ FLAG OF PLOT RESPONSE FUNCTION
      READ 1002,IPF,I
C
C **** RESPONSE FUNCTION
C
      CALL SPTIN(N,ICP)
      I1R=I1
      I2R=I1R+N-1
      DA=DA
      DB=DB
      DC=DC
      OLR=ICUT
C BACKGROUND CALCULATION
      DO 4 I=1,N
      G=I1P-I1+I
4     V(I)=(DA+G+DB)+G+DC
      IF(IPF.LE.0)
     -                GO TO 5
      PRINT 1005,(ICP(I),I=1,72)
      PRINT 1010,D1,DB,DC
      CALL PLOT(N,I1P,S,V,0)
C BACKGROUND SUBTRACTION
5     DO 6 I=1,N
6     S(I)=S(I)-V(I)
      CALL RESP(N)
      PRINT 1006,D0
      CALL FAN(M,N,BR)
      MN=REAL(BR(1))
      F1=(1.,0.)
      Q=(PO-FLOAT(I1))/N+2.*PI
      F10=CMPLX(COS(Q),SIN(Q))
      K=N/2
      DO 8 I=2,K
      F1=F1*F10
      BR(I)=(BR(I)*F1)/BR(1)
      L=N-I+2
8     BR(L)=CONJG(BR(I))
      F1=F1*F10
      BR(K+1)=(BR(K+1)*F1)/BR(1)
      BR(1)=(1.,0.)
C
C **** SPECTRUM TO BE DECONVOLUTED
C
20    CALL SPTIN(N,ICS)
      I2=I1+N-1
C SUBSTRACT BASE
      AG=(S(N)-S(1))/FLOAT(N-1)
      BG=S(1)
      DO 22 I=1,N
22    S(I)=S(I)-AG*(I-1)-BG
      CALL FAN(M,N,BS)
C CALCULATE AND WRITE COEFFICIENTS OF DECONVOLUTION
      DO 30 I=1,N
30    BD(I)=BS(I)/BR(I)
C CALCULATION OF MERIT
      V(1)=0
      K=N/2+1
      V(K)=0.
      Q=REAL(BS(K)*CONJG(BS(K)))/2.
      K=K-2
      DO 32 I=1,K
```

```
      J=K-I+2
      Q=Q+REAL(BS(J)*CONJG(BS(J)))/2.
      V(J)=STORNT(I)*SQRT(Q/FLOAT(I))
      L=K+2*I
      V(L)=V(J)
   32 CONTINUE
C CUT OFF FREQUENCY CALCULATION
      IFLAG=1ST
      IF(ICUT.LE.0)
     -                    GO TO 33
      JL=ICUT
      IFLAG=LAST
      GO TO 370
   33 Q=V(2)
      J=3
      K=N/2
      DO 36 I=3,K
      IF (V(I)-Q) 35,35,37
   35 J=I
      Q=V(I)
   36 CONTINUE
   37 JL=J
      IF(JL.GT.JLP)
     -                    JL=JLP
  370 CALL HEAD(1)
      PRINT 1007
      DO 34 I=1,N
      SR=REAL(BS(I))
      SI=AIMAG(BS(I))
      AS=BS(I)*CONJG(BS(I))
      AS=SQRT(AS)
      BR=REAL(BR(I))
      BI=AIMAG(BR(I))
      AR=BR(I)*CONJG(BR(I))
      AR=SQRT(AR)
      DR=REAL(BD(I))
      DI=AIMAG(BD(I))
      AD=BD(I)*CONJG(BD(I))
      AD=SQRT(AD)
   34 PRINT 1008,I,SR,SI,AS,BR,BI,AR,DR,DI,AD,V(I)
C TRUNCATION
      PRINT 1011
      K=N/2+1
      II=JL-1
      DO 38 I=2,II
      L=I+(K-1)*2
      Q=SIGMA(I,JL)
      BD(L)=BD(L)*CMPLX(Q,0.)
      DR=REAL(BD(L))
      DI=AIMAG(BD(L))
      AD=BD(L)*CONJG(BD(L))
      AD=SQRT(AD)
      PRINT 1009,I,DR,DI,AD
   38 BD(I)=BD(I)*CMPLX(Q,0.)
      K=JL+(K-JL)*2
      DO 40 I=JL,K
   40 BD(I)=(0.,0.)
      DO 41 I=1,N
   41 BS(I)=BD(I)
C INVERSE TRANSFORMATION OF DECONVOLUTED FUNCTION
      P=N
      CALL FFT(BD,N,-1.,P,W)
C RESTORE BASE
      DO 42 I=1,N
      S(I)=S(I)+AG*(I-1)+BG
   42 V(I)=REAL(BD(I))+AG*(I-1)+BG
      CALL HEAD(1)
```

```
      CALL PLOT(N,11,V,S,0)
      Q=AREA*NN*MON/10.**5
      P=TN*MONR/10.**5
      IF(Q-P) 20,20,80
80    Q=Q/P
      DX=A*DX*DDE/10000.
      CALL HEAD(2)
      PRINT 1016
      SUM=0.
      DO 92 I=1,N
      G=II-III+I
      G=(DA+G+DB)*C+DC
      C1=S(I)
      C2=V(I)
      S(I)=(S(I)-G)/Q/DX
      V(I)=(V(I)-G)/Q/DX
      SUM=SUM+V(I)*DX
      J=II+I-1
      E=J*A+B
      X=(E1+DL1-E)*DX*DE
92    PRINT 1017,J,E,C1,C2,X,V(I)
      SUM=SUM*AREA
      PRINT 1018,SUM
      CALL HEAD(2)
      PRINT 1018,SUM
      CALL PLOT(N,11,V,S,-1)
      GO TO 20
      END
```

```
      SUBROUTINE FAN(M,N,AA)
      COMPLEX AA
      DIMENSION AA(N)
      DIMENSION S(256),IS(256)
      COMMON II,IS,S,NF
C
      DO 10 I=1,N
2     P=S(I)
3     10  AA(I)=CMPLX(P,0.)
4     CALL FXT(AA,N,1.,1.,-1)
5     RETURN
      END
```

```
      SUBROUTINE SPTIN(N,IC)
C
C FORTRAN ROUTINE FOR READING OF SPECTRUM INTO ARRAY IS
C AND MAKING BACKGROUND SUBTRACTION FROM I1 TO I1+N
C
      DIMENSION IS(256),S(256),IC(72)
      COMMON I1,IS,S,NF
      COMMON /CONST/W1,W2,W3,RA,RB,DA,DB,AREA,MON,TN,NN,MONR,JL,IFLAG
      COMMON /CNST1/RC,DC,IBL1,IBL2,IBR1,IBR2,NCH,ICUT,I11
1000  FORMAT(14,72A1)
1001  FORMAT(F8.2,I8)
1002  FORMAT(7I5)
1003  FORMAT(8I5)
C READ CONSTANTS
C READ FIRST CHANNEL AND IDENTIFICATION OF SPECTRUM
10    READ 1000,NCH,(IC(I),I=1,72)
2     IF(NCH)12,20,20
3     12  STOP
C JOB DONE
4     20  READ 1002,I11,I1,IBL1,IBL2,IBR1,IBR2,ICUT
5         READ 1001,AREA,MON
6         READ 1003,(IS(I),I=1,NCH)
C FLOAT SPECTRUM
7         DO 30 I=1,NCH
8     30  S(I)=IS(I)
9         CALL BGFIT(NCH,I11,IBL1,IBL2,IBR1,IBR2,DA,DB,DC)
10        ID=I1-I11
11        DO 40 I=1,N
12        J=I+ID
13    40  S(I)=S(J)
14        RETURN
          END
```

```
      SUBROUTINE RESP(M)
C
C FORTRAN ROUTINE OF HANDLING RESPONSE SPECTRUM
C PERFORM BACKGROUND SUBTRACTION, NORMALIZATION AND ENERGY CALIBRATION
C
      DIMENSION IS(256),S(256)
      COMMON II,IS,S,NF
      COMMON /CAL/A,B,E1,E2,E3,P0,P1,P2,P3
      COMMON /CONST/W1,W2,W3,RA,RB,DA,DB,AREA,NON,TN,NN,NONR,JL,IFLAG
      COMMON /CNST1/RC,DC,IBL1,IBL2,IBR1,IBR2,NCH,ICUT,III
      DATA EPS/1.E-16/
C
C
C
      NONR=NON
C MAXIMUM SEARCHING
 2    J=1
 3    N=0
 4    DO 30 I=1,M
 5    IF(N-S(I))32,30,30
 6 32 N=S(I)
 7    J=I
 8 30 CONTINUE
 9    K=J+NF
10    J=J-NF
11    IF(J-1)34,36,36
12 34 J=1
13 36 IF(K-M)40,40,38
14 38 K=M
15 40 X0=0
16    X1=0
17    X2=0
18    X3=0
19    X4=0
20    Y1=0
21    Y2=0
22    Y3=0
23    DO 50 I=J,K
24    X0=X0+1
25    X1=X1+I
26    X2=X2+I**2
27    X3=X3+I**3
28    X4=X4+I**4
29    Y1=Y1+S(I)
30    Y2=Y2+S(I)*I
31 50 Y3=Y3+S(I)*I**2
32    D0=-(X4*Y2*X2-X3*Y3*X1*Y2+X2*X3*Y1-
     1X4*X1*Y1-Y3*X3*X0-Y2*X2**2)/
     22/(Y3*X2*X0+X3*X1*Y1-X2*Y2*X1-
     3Y3*X1**2-X3*Y2*X0-Y1*X2**2)+II-1
C ENERGY CALIBRATION
33    X0=W1+W2+W3
34    X1=W1*P1+W2*P2+W3*P3
35    X2=W1*P1**2+W2*P2**2+W3*P3**2
36    Y1=W1*E1+W2*E2+W3*E3
37    Y2=W1*E1*P1+W2*E2*P2+W3*E3*P3
38    D=X0*X2-X1**2
39    IF(ABS(D),LE,EPS)
40   -                          GO TO 99
41    A=(Y2*X0-X1*Y1)/D
42    B=(X2*Y1-Y2*X1)/D
43    RETURN
44 99 A=0
45    B=0
46    RETURN
      END
```

```
      SUBROUTINE HEAD(K)
      DIMENSION IS(256),S(256)
      COMMON I1,I2,S,NF
      COMMON /CAL/ A,B,E1,E2,E3,P0,P1,P2,P3
      COMMON /CONST/W1,W2,W3,RA,RB,DA,DB,AREA,MOM,TN,NN,MOMR,JL,IFLAG
      COMMON /CNST1/RC,DC,IBL1,IBL2,IBR1,IBR2,NCH,ICUT,I11
      COMMON /TEXT/ ICP(72),ICS(72),I2,I1R,I2R
 1003 FORMAT(1H1,22X,35HSPECTRUM DECONVOLUTION USING FFT//)
 1004 FORMAT(24H SPECTRUM DECONVOLUTED: ,72A1)
 1005 FORMAT(24X,5HFROM:,I4,4H TO:,I4,9H CHANNELS)
 1006 FORMAT(/24H      RESPONSE SPECTRUM: ,72A1)
 1007 FORMAT(11X,22HBACKGROUND PARAMETERS:,F8.4,2F8.2)
 1008 FORMAT(6X,23HRESPONSE PEAK POSITION:,F8.2)
 1009 FORMAT(/11X,18HCUT OFF FREQUENCY:,I4,2X,A1)
 1010 FORMAT(11X,21HENERGY CALIBRATION E:,8X,3F8.2/
     *30X,2HP:,4F8.2/20X,13HCOEFFICIENTS:,2E12.4)
 1019 FORMAT(11X,25HCONVOLUTION CALIBRATION,2X,
     *4HAREA,6X,1HM,6X,3HSUM,4X,5HMONIT/25X,
     *8HMONITOR:,F8.2,F8.2,F8.2/24X,9HSPECTRUM:,F8.2,16X,I8)
      PRINT 1003
    2 PRINT 1004,(ICS(I),I=1,72)
    3 PRINT 1005,I1,I2
    4 PRINT 1007,P1,P2,DC
    5 PRINT 1006,(ICP(I),I=1,72)
    6 PRINT 1005,I1R,I2R
    7 PRINT 1007,RA,RB,RC
    8 PRINT 1008,P0
    9 PRINT 1009,JL,IFLAG
   10 IF(K.EQ.1)
   11 -          RETURN
   12 PRINT 1010,E1,E2,E3,P0,P1,P2,P3,A,B
   13 PRINT 1019,TN,NN,MOMR,AREA,MOM
   14 RETURN
      END
```

```
      SUBROUTINE BGFIT(N,M1,IBL1,IBL2,IBR1,IBR2,A,B,C)
C
C
      DIMENSION IS(256),S(256)
      COMMON I1,I5,S,MP
      DATA EPS/1.E-10/
C
      X0=0
      X1=0
      X2=0
      X3=0
      X4=0
      Y0=0
      Y1=0
      Y2=0
      W=0.001
      DO 10 M=IBL1,IBL2
      J=M-I1+1
  101 X0=X0+W
      X1=X1+W*J
      X2=X2+W*J**2
      X3=X3+W*J**3
      X4=X4+W*J**4
      Y0=Y0+W*S(J)
      Y1=Y1+W*S(J)*J
   10 Y2=Y2+W*S(J)*J**2
      DO 12 M=IBR1,IBR2
      J=M-I1+1
  101 X0=X0+W
      X1=X1+W*J
      X2=X2+W*J**2
      X3=X3+W*J**3
      X4=X4+W*J**4
      Y0=Y0+W*S(J)
      Y1=Y1+W*S(J)*J
   12 Y2=Y2+W*S(J)*J**2
      D=X4*X2*X0+X3*X1*X2*2*X3*X1-X4*X1**2-X3**2*X0-X2**3
      IF(ABS(D).LE.EPS)
     -                    GO TO 99
      A=(Y2*X2*X0+X3*X1*Y0+X2*Y1*X1-Y2*X1**2-X3*Y1*X0-X2**2*Y0)/D
      B=(X4*Y1*X0+Y2*X1*X2+X2*X3*Y0-X4*X1*Y0-Y2*X3*X0-X2**2*Y1)/D
      C=(X4*X2*Y0+X3*Y1*X2+Y2*X3*X1-X4*Y1*X1-X3**2*Y0-Y2*X2**2)/D
      RETURN
   99 A=0
      B=0
      C=0
      RETURN
      END
```

```
      SUBROUTINE PLOT (N,Y1,V,S,ZERO)
      DIMENSION V(256),S(256),LINE(104)
      DATA ISP,MN,LI,LT,LO/1H ,1H-,1HI,1H*,1HO/
 1010 FORMAT(//25H    DECONVOLUTED  CHANNEL,80X,
     *23HCOUNTS IN RELATIVE UNIT)
 1011 FORMAT(//26H  DECONV MEASURED  CHANNEL,78X,
     *24HCOUNTS IN RELATIVE UNITS)
 1012 FORMAT(24X,1H0,9X,2H10,8X,2H20,8X,2H30,8X,
     *2H40,8X,2H50,8X,2H60,8X,2H70,8X,2H80,8X,2H90,7X,3H100)
 1013 FORMAT(24X,40H+---------+---------+---------+---------+,
     *50H---------+---------+---------+---------+---------+,
     *14H---------+---)
 1014 FORMAT(1X,F8.2,1X,I6,2X,104A1)
 1015 FORMAT(1X,E14.4,1X,2X,104A1)
      P=0
    2 IF(ZERO) 12,20,20
    3 12  P=V(1)
    4     DO 14 I=1,N
    5     IF(P.GT.V(I))
    6    -              P=V(I)
    7 14  CONTINUE
    8 20  Q=V(1)
    9     DO 22 I=1,N
   10     IF(Q.LT.V(I))
   11    -              Q=V(I)
   12 22  CONTINUE
   13     D=(Q-P)/100.
   14     IF(D.EQ.0)
   15    -          RETURN
   16     IF(ZERO) 23,24,23
   17 23  PRINT 1010
   18     GO TO 25
   19 24  PRINT 1011
   20 25  PRINT 1012
   21     PRINT 1013
      C SET UP PLOT SPINC
   22     DO 80 I=1,N
   23     DO 30 J=2,104
   24 30  LINE(J)=ISP
   25     LINE(1)=LI
   26     LINE(104)=LT
   27     IF(ZERO.LT.0)
   28    -              GO TO 42
   29     Q=S(I)
   30     IF (Q.LT.0)
   31    -          Q=-Q
   32     K=(S(I)-P-SQRT(Q))/D+1.499
   33     L=(S(I)-P+SQRT(Q))/D+1.5
   34     IF(L-1) 70,42,32
   35 32  IF(K-1) 33,34,34
   36 33  K=1
   37 34  IF(K-104) 35,35,70
   38 35  IF(L-104) 37,37,36
   39 36  L=104
   40 37  DO 40 J=K,L
   41 40  LINE(J)=MN
   42     LINE(K)=LI
   43     LINE(L)=LT
   44 42  K=(S(I)-P)/D+1.5
   45     IF(K-1) 70,44,44
   46 44  IF(K-104) 46,46,70
   47 46  LINE(K)=LO
   48 70  K=(V(I)-P)/D+1.5
```

```
49          IF(K-1) 72,72,74
50    72    K=1
51    74    LINE(K)=IAST
52          J=11+121
53          K=S(I)+.5
54          IF(ZERO) 76,78,76
55    76    PRINT 1015,V(I),J,(LINE(L),L=1,104)
56          GO TO 80
57    78    PRINT 1014,V(I),K,J,(LINE(L),L=1,104)
58    80    CONTINUE
59          PRINT 1013
60          PRINT 1012
61          RETURN
            END
```

```
            FUNCTION SIGMA(K,M)
      C
      C LANCZOS-SIGMA FACTOR
      C
            P=K
      2     Q=M
      3     P=P*3.141593/Q
      4     SIGMA=SIN(P)/P
      5     RETURN
            END
```

```
            FUNCTION STUDNT(K)
      C
      C FORTRAN FUNCTION OF STUDENT T FACTOR
      C
            COMMON /ST/TTAB(30)
      C
            IF(K)10,10,20
      2     10    STUDNT=0
      3           RETURN
      4     20    I=K
      5           IF(I-30)24,24,22
      6     22    I=30
      7     24    STUDNT=TTAB(I)
      8           RETURN
                  END
```

REFERENCES

[1] Duwez P.: Structure and Properties of Glassy Metals. Annual Rev. Materials Sci. 6, 83-117, /1976/

[2] Mendelsohn L.I., Nesbitt E.A., Bretts G.R.: Glassy Metal Fabric: A Unique Magnetic Shield Proc. IEEE/AIP Joint Intermag Conference, Pittsburgh, June 17, /1976/

[3] Nagy Á.Z., Bogáncs J., Gyulai J., Csőke A., Nazarov V., Seres Z., Szabó A., Yasvitsky Yu.: Determination of Boron Range Distribution in Ion-implanted Silicon by the $^{10}B/n, \alpha/^{7}Li$ Reaction. J. Radioanal. Chem. 38, 19-27 /1977/

[4] Ziegler J.F., Chu W.K.: Stopping Cross Section and Backscattering Factors for ^{4}He Ions in Matter Z = 1-92, $E/^{4}He/$ = 400-4000 keV. Atomic Data and Nuclear Data Tables 13, 463, /1974/

[5] Ziegler J.F.: Helium Stopping Powers and Ranges in All Elemental Matter. Vol. 4. The Stopping and Ranges of Ions in Matter. Pergamon Press, N.J. /1978/

[6] Lánczos C.: Applied Analysis, Prentice-Hall. Englewood Cliffs, N.J. /1961/

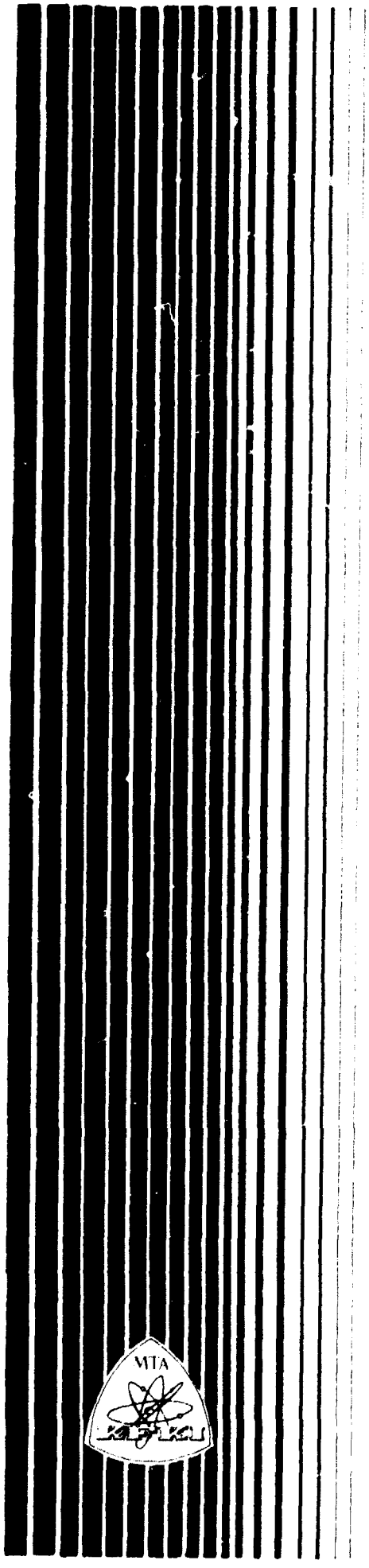

Kiadja a Központi Fizikai Kutató Intézet
Felelős kiadó: Krén Emil
Szakmai lektor: Konczos Géza
Nyelvi lektor: Harvey Shenker
Példányszám: 250 Törzsszám: 79-946
Készült a KFKI sokszorosító üzemében
Budapest, 1979. december hó